Optica Applicata, Vol. XXV, No. 3, 1995

On a consequence of the Young–Rubinowicz model of diffraction phenomena in holography

P. V. Polyanskii, G. V. Polyanskaya

Department of Correlation Optics, Chernovtsy University, ul. Kotsyubinsky 2, 274012 Chernovtsy, Ukraine.

Imaging properties of a recorded near-field diffraction are predicted on the basis of Young's interpretation of diffraction phenomena. Physical adequacy of the approach of Young–Rubinowicz is justified experimentally by a reconstruction of holographic images from diffraction patterns. It is shown that Young's holography proposed here is an efficient method of contour imaging.

1. Introduction

Diffraction phenomena (such as a straight edge diffraction, diffraction by an aperture and by a screen) are usually considered on the basis of the Huygens–Fresnel principle. In accordance to this model, a diffraction pattern is calculated as a result of an interference of partial signals originating from fictious secondary sources positioned in the diffraction aperture and alloted (arbitrarily to a certain extent) by some amplitudes, phases, and inclination coefficients. These allowances are in part based on the framework of Kirchhoff's scalar diffraction theory [1]. Nevertheless, the diffraction paradigm of Fresnel is a receipt for a calculation of a diffraction pattern, rather than a universal way of understanding of diffraction phenomena. It has been noted more than once (see, for example, [2], [3]) that the expedient choice of a model for a description of diffraction is dictated by specific features of a concrete problem which has been solved.

The alternative (and very convincing) explanation of diffraction, put forward by Young and formalized mathematically by RUBINOWICZ [4], operates with two physical irradiators only, such as a primary source and a retransmitting edge of the diffraction screen. Contrary to the Fresnel–Kirchhoff model, considering a diffraction as a result of any integral transform of the single wave which fills an aperture, the Young–Rubinowicz (YR) model states that a diffraction pattern originates from interference of an undisturbed primary wave (existing at the region of light only) and a wave retransmitted by the knife-edge which propagates both in the area illuminated by the primary wave and in the geometrical shadow area. Under certain suppositions concerning properties of an edge wave discussed in [1], [5], approaches of Fresnel and Young turn out to be quite equal (at any rate, within the bounds of justice of the Kirchhoff theory). Existence of a wave propagating from the knife-edge into the area of geometrical shadow has been experimentally proved by KALASHNIKOV [6].

In the present paper, one consequence of the YR model of diffraction will be developed and experimentally verified. This consequence consists in a supposition that the near-field diffraction pattern, being recorded photographically without supplementary reference wave, as a metter of fact, is a hologram of the edge of the diffraction screen. The same affirmation has been recently formulated by MULAK [7]. Such special type of a hologram will be here referred to as "Young's hologram" (YH). As it will be shown, Young's holography is an efficient means of contour imaging.

2. Diffraction pattern is a hologram

2.1. Background

Let us consider a knife-edge diffraction on the basis of the YR model, the due illustration being given in Figure 1. Perturbance $U(P)$ at the running point of the observation plane S at the region of light is calculated as a result of an interference between the primary spherical wave

$$U_g(P) = \frac{U(P_0)}{r_g} \exp(-ikr_g) \tag{1}$$

and the cylindrical wave retransmitted by the knife-edge

$$U_d(P) = \int \frac{U(D,\Phi)}{r_d} \exp(-ikr_d) dl. \tag{2}$$

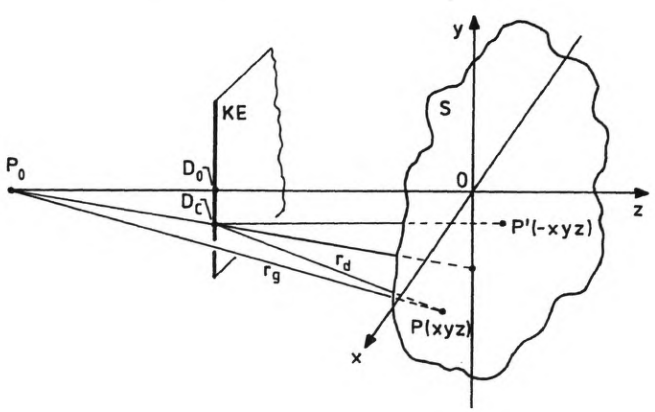

Fig. 1. Notations: $x < 0$ is the geometrical shadow, $x > 0$ is the region of light, where Young's hologram is recorded

For the present consideration, there is no necessity to detail the features of an amplitude function $U(D,\Phi)$. Note only that it is characterized with an angular dependence given by the so-called "Rubinowicz representation" [5]. It depends, in general, on the polarization of the disturbing wave as well as on the knife-edge

material, and integration is performed on the contour of the diffraction screen. We shall restrict our consideration to the scalar case and use the fact that, according to the stationary phase principle [1], [3], the problem is reduced to the plane one, *i.e.*,

$$U_d(P) = \frac{U(D_c, \Phi)}{r_d} \exp(-ikr_d) \tag{3}$$

where D_c refers to the critical point at the edge of a diffraction screen lying in the plane, which has been determined by points P_0, P and P' (P' is a mirror image of the point P from a bound of geometrical shadow). An intensity distribution at the plane S has the form

$$I(P) = |U_g + U_d|^2 = |U_g|^2 + |U_d|^2 + U^*(P_0)U(D_c, \Phi)\frac{\exp\{ik(r_g - r_d)\}}{r_g r_d} + U(P_0)U^*(D_c, \Phi)\frac{\exp\{-ik(r_g - r_d)\}}{r_g r_d}. \tag{4}$$

Supposing that conditions of a linear holographic recording [8] are satisfied, we shall register photographically an intensity distribution (4). As a result, we receive a photogram with an amplitude transmittance

$$T_a(P) \sim I(P). \tag{5}$$

Such a photogram of the knife-edge diffraction can be considered as a hologram of the edge of a diffraction screen, where the primay wave $U_g(P)$ plays the role of the reference one. Indeed, if the knife-edge is removed, and the developed photoplate is illuminated with the wave (1), immediately behind the plane S we receive

$$\{T_a\}U_g \sim [|U_g|^2 + |U_d|^2]U_g(P) + \frac{|U_g|^2}{r_g^2}U_d(P) + \frac{U_g^2}{r_g^2}\exp\{-ik2r_g\}U_d^*(P). \tag{6}$$

It is easy to recognize the basic equations of holography in expressions (4)–(6). The first term of Eq. (6) describes a forward diffracting wave of the readout source; the second and the third ones are diffracting waves of the plus–minus first orders forming the main and the conjugate images of the knife-edge, respectively.

It has been emphasized that the possibility for the part of diffraction wave to be reconstructed by any of its other parts is anything but obvious, while a diffraction phenomenon is considered on the basis of the Huygens–Fresnel principle. What is more, according to one of the most fundamental interpretations of the optical holography principle [9] explaining the imaging properties of a hologram as a manifestation of its associative properties, the effective mutual interference modulation of partial exposing waves at the registration plane is needed for a consequent reconstruction of the part of a recorded wave by its other part: information about an amplitude and phase of the associative pair terms is "remembered" just in a substructure of the recorded intermodulation pattern. As a consequence, the Fresnel referenceless hologram can be generated for diffuse objects only which are characterized by large (in the wavelength scale) optical

inhomogeneities. That conclusion has been recently confirmed in [10] for the most general case of the quadratic hologram based associative memory.

Going back to the knife-edge diffraction, we can ascertain the fact that in the YR model only an optical inhomogeneity (the knife-edge) figures clearly playing the role of an optical retransmitter responding to an interference modulation of the forward wave at the registration plane. Of course, the YH discussed here is not equal to a hologram of a diffracting wave which is the one recorded using supplemental reference beam and which reconstructs the complete field: $U(P) = U_g(P) + U_d(P)$ at the plane S. In our case, in contrast, the wave playing the role of a reference one with regard to the edge wave $U_d(P)$ is found inside of the diffracting field itself. This means that both amplitude and phase information is retained in the spatial-frequency structure of the recorded diffraction pattern. Thus, the necessary and sufficient condition is satisfied for forming the holographic image of the contour of the diffraction screen.

2.2. Imaging properties of Young's hologram

The YR model differs from the Fresnel one in explanation of the nature of a diffraction pattern rather than in predictions concerning its detailed structure. That is why, features of the YH as well as properties of an image reconstructed by it can be discussed on the basis of calculation using Fresnel's integrals. According to such calculation, an intensity distribution of the diffraction field is given by the expression [11]

$$|U(\omega)|^2 = 0.5\{[0.5 + C(\omega)]^2 + [0.5 + S(\omega)]^2\}|U_g|^2 \tag{7}$$

where $C(\omega)$ and $S(\omega)$ are Fresnel's integrals, $\omega = (\lambda f)^{-1}\pi x^2$ and $f = R_g R_d/(R_d - R_g)$, where $R_g = |P_0 0|$ and $R_d = |D_0 0|$ in notations of Fig. 1. As it is well known, the function $|U(\omega)|^2$ has an oscillation form with decreasing amplitude in the neighbourhood of an intensity magnitude of a nondisturbed wave $|U_g|^2$, which is realized in absence of a diffraction screen.

Evaluation of an energy efficiency of the YH, which is a diffraction grating with varying modulation depth and with varying spacing, is the key problem. Since there exists no general method of diffraction efficiency estimation for such grating, we propose the following procedure of evaluation of the hologram efficiency. The diffraction efficiency is defined as a ratio of the power diffracted into the 1-st diffraction order to the power incident during reconstruction

$$\eta = \frac{P_{\text{image}}}{P_{\text{readout}}}. \tag{8}$$

Let us consider the positive transparency with the transmittivity along x-axis proportional to the intensity distribution given by (7). The width of this transparency Δy is small and localized near of the origin of the coordinate system 0 (see Fig. 1). Our considerations restricts to the paraxial region. Dividing hologram onto zones according to the periods of the recorded diffraction grating, we obtain for n-th zone

$$\eta_n \approx \frac{P_n}{I_0 \Delta x_n \Delta y} \tag{9}$$

where: I_0 is the intensity of incident light, Δx_n is the dimension of n-th zones.

The spatial frequency μ_n and the spatial period satisfy the relation

$$\mu_n \Delta x_n = 1. \tag{10}$$

Taking into account

$$\Delta \Phi \approx \left(\frac{\partial \Phi}{\partial x}\right) \Delta x \tag{11}$$

(where Φ is given by the exponent argument in Eq. (4)), we find

$$\mu_n = \left(\frac{\partial \Phi}{\partial x}\right)_n = (\lambda f)^{-1} x_n \tag{12}$$

where f is defined in the text below Eq. (7).

Expanding the phase Φ into power series with respect to x and neglecting the terms of higher orders, we obtain

$$x_n \sim n^{1/2}. \tag{13}$$

The power originating from n-th zone may be evaluated as

$$P_n \approx \eta_n I_0 \Delta x_n \Delta y = I_0 \eta_n \mu_n^{-1} \Delta y. \tag{14}$$

On the other hand, the diffraction efficiency is equal to [12]

$$\eta_n = k \frac{m_n^2}{16} \tag{15}$$

where k is the slope of the exposure characteristics of the photographic material, m_n is the depth of modulation.

Combining (14) and (15) we obtain

$$P_n \approx k I_0 \frac{m_n^2}{16} \mu^{-1} \Delta y. \tag{16}$$

The depth of modulation m_n is equal to the contrast of the recorded interference pattern (linear approximation). The mean contrast $\langle V_n \rangle = \langle (I_{max} - I_{min})/(I_{max} + I_{min}) \rangle_n$ has been determined for each n by means of quadratic interpolation from envelopes of the function $|U(\omega)|^2$.

The power coming from n-th period with respect to that originating from the first zone is

$$\frac{P_n}{P_1} \approx \frac{m_n^2 \mu_1}{m_1^2 \mu_n} \sim \frac{\mu_1}{m_1^2} \frac{m_n^2}{n^{1/2}}, \tag{17}$$

$\frac{m_1^2}{\mu_1}$ is equal to .42. Calculating m_n for $n = 1, 2, \ldots, 25$ we obtain the dependence

P_n/P_1 shown in Fig. 2 (black circles). An approximation curve (dashed line in Fig. 2) is found as

$$\frac{P_n}{P_1} = n^{-e^{1/2}}. \tag{18}$$

The total power in the image is evaluated as

$$P_{\text{im}} = \sum_{n=1}^{\infty} P_n = P_1 \zeta(e^{1/2}) \tag{19}$$

where $\zeta(e^{1/2})$ is zeta-function of Riemann [13] defined as

$$\zeta(e^{1/2}) = \sum_{n=1}^{\infty} \frac{1}{n^{e^{1/2}}}. \tag{20}$$

(Of course, the sum in infinite limits means the violation of the paraxiality assumption).

Returning to the total efficiency (within paraxial approximation)

$$\eta = \frac{k}{16} \frac{\sum_{n=1}^{N} m_n^2 \mu_n^{-1}}{\sum_{n=1}^{N} \Delta x_n} = \frac{k}{16} \frac{\sum_{n=1}^{N} m_n^2 \mu_n^{-1}}{x} \tag{21}$$

where x is the size of hologram in the x-direction.

The sum of the infinite series (20) is approximately equal to 2.2 [14], so that we finally have: $P_{\text{image}}(\times 100\%) \approx 0.92\%$. This result shows that an energy efficiency of the YH is equal to an efficiency of amplitude harmonic hologram-grating obtained under beam ratio 1:25. Extrapolation on the phase-only recording realized with the same beam ratio gives an estimate of efficiency of the phase YH about 3.6%.

The main condition of a linear holographic recording, provided that Eq. (5) is justified, as exposure is varied within large limits, is the following: $|U_g|^2$ must be, at the least, three times larger than $|U_d|^2$ [15]. Since that condition is satisfied over all the area of superposition of the forward propagating wave and the wave retransmitted by the knife-edge (perhaps, excluding the nearest vicinity of the shadow border), then the linear approximation of the holographic theory adopted in Sect. 2.1 is quite adequate. Thus, we can hope that the YH will form a high-quality image of an edge of the diffraction screen with a low level of nonlinear distortions. We draw attantion to the fact that although a phase hologram is nonlinear in principle because of the saturation of the phase-exposing characteristics [8], [10], it is considered that a nonlinearity of phase recording can be neglected if phase deviations do not exceed 0.2 rad [16]. Holographic investigation of the phase distribution in a knife-edge diffraction pattern as well as comparison of its results with Cornu's spiral based calculation show that phase deviations lie in bounds corresponding to the linear approximation [17]. Thus, the phase YH is also a linear one. Hence, the typical holography dilemma of choosing diffraction efficiency and quality of a reconstructed image is solved in favour of the latter in Young's holography.

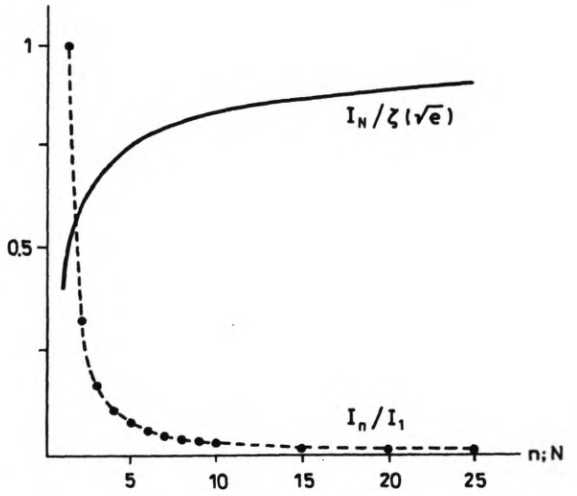

Fig. 2. Energy efficiency of Young's hologram. Relative contribution of the YH periods into intensity of a reconstructed image are designated by the points. The dashed curve shows an envelope of an approximate dependence $I_n \approx n^{-e^{1/2}}$. The solid curve shows a relative intensity of a reconstructed image as a function of number N of corresponding periods

Although the above estimations of the YH efficiency are based on summation over $n = \overline{1,\infty}$, the direct calculation of a reconstructed image intensity *vs.* the number N of corresponding periods $I_N = \sum_{n=1}^{N} I_n$, where $I_n \sim P_n$, which is defined by Eqs. (14) or (18), shows that the biggest share of energy contributing to image formation (about 90%) is delivered by the first 25 periods, see the curve $I_N/\zeta(e^{1/2})$ in Fig. 2. A real YH appears to be small-angled and, as a consequence, location and scale of the main and the conjugate images are justifiably predicted by relationships of paraxial optics of a hologram [18]. So, if the wavelength of recording irradiance is equal to the wavelength of the readout one, then location of the main image (L_1) and of the conjugate image (L_2), in respect to the point 0 in Fig. 1, is given by the expression

$$L_{1,2} = Rf/(f \mp R) \tag{22}$$

where R is the distance from point 0 to the readout source. The lateral image magnification (for diffraction screen with the form more complicated than the half-plane) is given by the relationship [18], [19]

$$H_{1,2} = \pm L_{1,2}/R_d. \tag{23}$$

Contour imaging of diffraction screens subordinate to Eqs. (22) and (23) must be considered as an experimental confirmation of the existence of holographic properties for the recording of the near-field diffraction.

3. Experimental verification

3.1. Experimental setup and conditions of edge detection

The experiment illustrating the YH imaging properties is performed by optical arrangement presented in Fig. 3. Irradiance of a laser L, passing through microobjective and spatial filter, diffracts on the knife-edge KE and forms at the registration plane RP an illumination distribution which has been registered on a photoplate PP. The developed photoplate is the YH of a knife-edge.

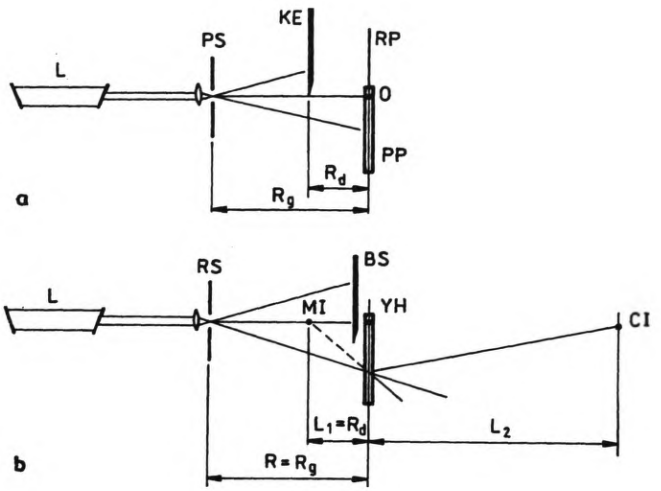

Fig. 3. Experimental setup: **a** – recording stage, **b** – readout stage. L – laser, PS – primary source = microobjective + spatial filter, KE – knife-edge, PP – photoplate, RP – registration plane, RS – readout source, YH – Young's hologram, BS – blocking screen, MI – main image, OP – observation plane, CI – conjugate image

The YH can be readout at the same setup if a knife-edge is removed, and a photoplate is illuminated with a spherical wave from the primary source. We expect to observe through a hologram the main image MI of a knife-edge at the original position, as it has been predicted in Sect. 2. However, as the efficiency of the YH is very low (both amplitude hologram and phase one), it is difficult to detect the main bright-field image. Evidently, because of low contrast of a knife-edge diffraction and low efficiency of the YH, imaging properties of a diffraction pattern had not been noticed earlier.

More favourable conditions of a knife-edge detection are realized for a conjugate image which can be formed behind the hologram, as it is predicted by Eq. (22) (L_2 being measured from the point 0 is negative), when distances R_g and R_d are properly chosen. Then, a real dark-field conjugate image CI can be observed if the part of the powerful reading beam corresponding to an area of geometrical shadow is cut off by a blocking screen BS, as it has been shown in Fig. 3b. Of course, such a screen forms a diffraction pattern itself which may overlap with the reconstructed

conjugate image. Distortion effects of a blocking screen on the conjugate image can be reduced to minimum if the screen is placed below the point 0 and, in such a way, several first periods of the YH are blocked. The choice of the position of the screen BS is determined in the following considerations. First, the distributed feature of a holographic recording causes its excessive nature [8], which manifests itself in the well known fact that any part of the hologram reconstructs a whole image of an object. In the YH such property is reduced to a one-dimensional distributivity, so that an information about the critical point D_c (see Fig. 1) is registered along the axis $x > 0$, if y associated with the point D_c is the constant. Second, according to the classification of holographic setups in terms of imaging systems [20], [21], the YH is the aperture one (contrary to an image hologram which is the field one). That is why, blocking of the readout wave at the pupil of the imaging system, *i.e.*, at the YH plane, as it is shown in Fig. 3b, allows avoiding a vignetting of imaging beams which would take place in any other position of the blocking screen. In our case, the whole wave diffracted by the opened area of the YH takes part in the reconstruction of the conjugate image.

Note that a "twin" conjugate image, having no bearing to any complementary information with respect to the main one and hindered to Gabor in his original in-line holography setup, has been recently used for realization of an exceptionally effective method of a quadratic-hologram based associative data reconstruction [22]–[25]. The method of edge detection of a diffraction screen described here is, once more, a useful application of a conjugate image. A similar technique has been used earlier by Thompson for the Fraunhofer hologram based holographic microscopy [26].

3.2. Results

Our experiments on observation of imaging properties of the YH have been performed under the following conditions: $\lambda = 0.63$ μm, $R_0 = 80$ cm, $R_d = 20$ cm, then (if $R = R_0$) $L_2 = -40$ cm. Diffraction pattern has been recorded using holographic photoplates VRL (developer D-19).

The first experiment was carried out using a half-plane bounded in the profile form. An object, a diffraction pattern (considered here as the YH), and reconstructed conjugate images are shown in Fig. 4, retaining relative scales. A large-scale irregular pattern superimposing with a fine diffraction structure of interest (see Fig. 4b) has been caused by higher-order reflections from bounds of a photolayer substrate. It has no effects on the YH imaging properties. In Figure 4c, the conjugate edge image, which has been reconstructed with the beam bounded by a strict half-plane, is shown. Zero diffraction order is here observed close to contour image. When the photogram shown in Fig. 4d was obtained, zero order diffraction has been filtered by an opaque screen positioned immediately in front of the conjugate image plane. Comparison of scales of an object and a reconstructed image confirms predictions of the paraxial theory of a hologram very well.

The example of a conjugate image reconstruction for a closed contour is illustrated in Fig. 5. Diameter of a circle diffraction aperture was 1 cm. This

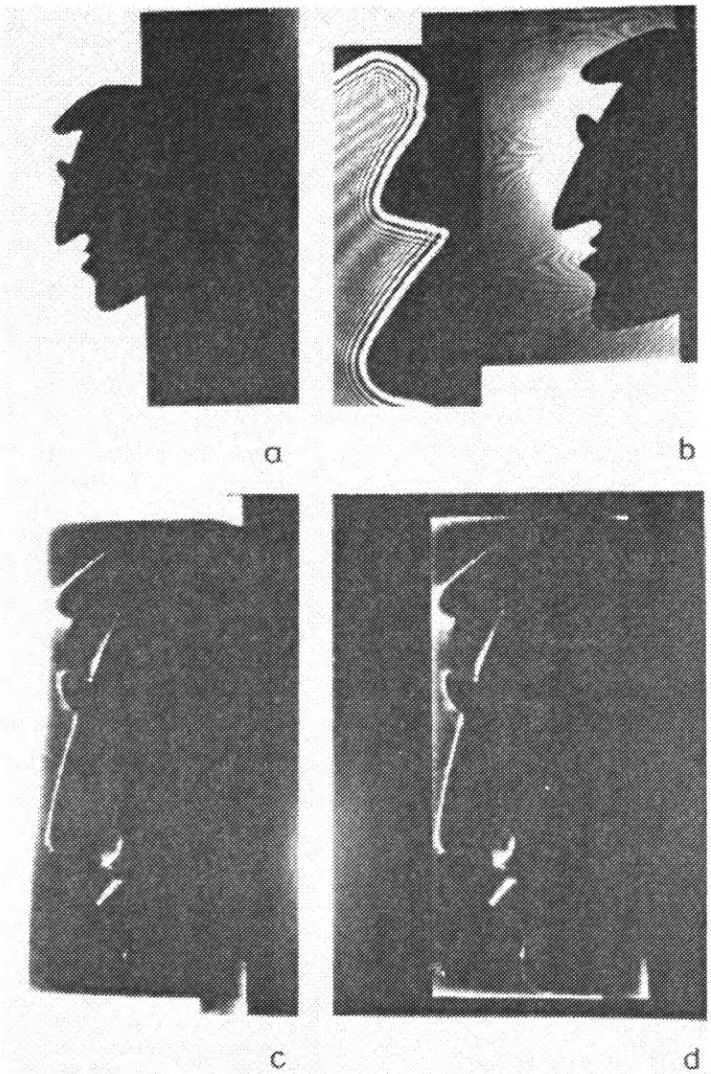

Fig. 4. Detection of a profiled edge of a half-plane. **a** — diffraction screen, **b** — Young's hologram, **c** — conjugate image with a zero diffraction order, **d** — dark-field conjugate image

corresponds to recording of a near-field diffraction under geometrical and wavelength experimental conditions noted above. Contour imaging corresponding to original diffraction screen confirms an objective edge detection free from a readout beam configuration.

Demonstrations represented above show the recording of a near-field diffraction pattern reconstructing a detailed image of the diffraction screen edge. Thus, the YH appears to be a simple means of solving in practice the important task of contour imaging which, at present, attracts significant efforts, particularly in investigations of the so-called high-level functionality of computational models of optical neural networks [27].

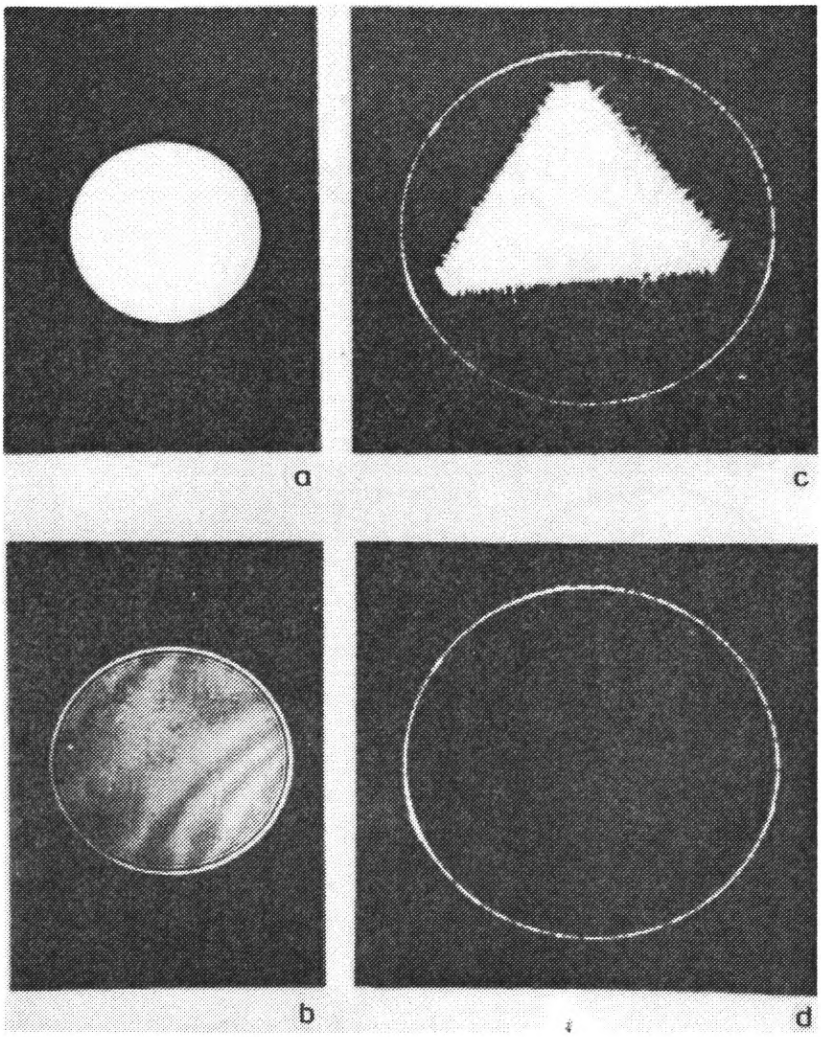

Fig. 5. Detection of a closed contour of the circle diffraction aperture. **a** – diffraction screen, **b** – Young's hologram, **c** – conjugate image with a zero diffraction order, **d** – dark-field conjugate image

4. Conclusions

Interference and diffraction phenomena lying at the foundation of the holography method are traditionally considered on the basis of the Huygens–Fresnel principle. However, diffraction phenomena as well as the holography method turn out to be more diverse in their manifestations than it concludes from any partial model used. That is why, they can serve in development and verification of the alternative models.

Episodic attempts of the holographic investigation of diffraction pattern had been undertaken earlier, especially in the initial phase of development of laser

holography [17], [28]. Such investigations, however, were carried out irrespective of concrete models explaining the origin of a diffraction pattern. The results presented here show that a heuristic efficiency of the diffraction paradigms of Fresnel and Young is not quite equal. Proceeding from Young's notion only, an existence of imaging properties of recorded near-field diffraction can be recognized. Experimental verification of this prediction consists in a holographic reconstruction of the wave complex-conjugated to one propagating from the screen edge. As a result, the conjugate edge image is formed. Thus, the existence of the edge wave at the region of light finds an unambiguous experimental evidence.

In conclusion, we shall point out some more potential possibilities for experimental background of the YR model of diffraction using a holographic method. "Holographic" features of this model prompt conditions when departures (obviously small) of experimental results from predictions of an essentially scalar diffraction theory of Fresnel–Kirchhoff can be detected. Particularly, a holographic investigation of the edge wave indicatrix, determined analytically by the Rubinowicz representation, is of interest, as well as fine dependence of a diffraction in the nearest neighbourhood of the bound of geometrical shadow on the primary wave polarization and substance of a diffraction screen.

References

[1] BORN M., WOLF E., *Principles of Optics*, Pergamon Press, Oxford 1969.
[2] KARCZEWSKI B., WOLF E., J. Opt. Soc. Am. **56** (1966), 1207.
[3] VAGANOV R. B., KATSENELENBAUM B. Z., *Principles of the Diffraction Theory* (in Russian), [Ed.] Nauka, Moscow 1982.
[4] RUBINOWICZ A., Nature **180** (1957), 160.
[5] SOMMERFELD A., *Vorlesungen über theoretische Physik*, Band 4 *Optik*, Academic Press, New York 1954.
[6] KALASHNIKOV A., J. Russ. Phys. Chem. Soc. **44** (1912), 133.
[7] MULAK G., Abstracts of the IC *Diffractometry and Scatterometry*, May 24–28, Warsaw 1993, p. 48.
[8] COLLIER R. J., LIN L., BURCKHARDT C., *Optical Holography*, Academic Press, New York 1971.
[9] COLLIER R. J., Spectrum **3** (1966), 67.
[10] POLYANSKII P. V., PhD Thesis, Belorussian Academy of Sciences, Minsk 1991.
[11] LANDAU L. D., LIFSHITZ E. M., *Course of Teoretical Physics*, Vol. 2, *Theory of Fields* (in Russian), [Ed.] Nauka, Moscow 1988.
[12] MILER M., *Golografiya* (in Russian), [Ed.] Mashinostroenie, Leningrad 1979.
[13] ARFKEN G., *Mathematical Methods for Physicists*, Academic Press, New York, London 1970.
[14] JANKE E., EMDE F., LOSCH F., *Tafeln hoherer Funktionen*, Teubner Verlag., Stuttgart 1960.
[15] SEMIONOV G. B., DENISYUK YU. N., SAVOSTIANENKO N. A., *Proc. Third USSR School on Holography*, January 25–30, 1971, Leningrad, p. 113.
[16] CATHEY W. T., J. Opt. Soc. Am. **56** (1966), 1167.
[17] HARRIS J. S., GIVENS M. P., J. Opt. Soc. Am. **56** (1966), 862.
[18] KOVALSKII L. V., POLYANSKII V. K., TIMOFEEV V. B., Quantum Electron. (Kiev) **3** (1967), 74.
[19] GOODMAN J. W., *Introduction to Fourier Optics*, McGraw-Hill Co., New York 1968.
[20] POLYANSKII V. K., KOVALSKII L. V., *Proc. Third USSR School on Holography*, January 25–30, 1971, Leningrad, p. 53.
[21] ZAKSHETSKAYA T. YA., KOVALSKII L. V., POLYANSKII V. K., Opt. Spectrosc. **37** (1974), 171.
[20] POLYANSKII P. V., Opt. Spectrosc. **65** (1988), 435.
[21] POLYANSKII P. V., Opt. Spectrosc. **72** (1992), 671.

[24] POLYANSKII P. V. SPIE **2108** (1993), 435.
[25] POLYANSKII P. V., Proc. SPIE **1991** (1994), 99.
[26] THOMPSON B. J., *Fraunhofer Holograms*, [In] *Handbook of Optical Holography*, [Ed.] H. J. Caulfield, Academic Press, New York 1979, Sect. 4.2.
[27] AGHADJAN H. K., SCHAPER C. D., KAILATH T., Opt. Eng. **32** (1993), 828.
[28] HART H. E., SCRANDIS J. B., MARK R., J. Opt. Soc. Am. **56** (1966), 1018.

Received August 8, 1994
in revised form July 10, 1995